COMMUNICATION

ChemComm
www.rsc.org/chemcomm

Synthesis and characterization of multiferroic $BiFeO_3$ nanotubes†

Tae-Jin Park,[a] Yuanbing Mao[a] and Stanislaus S. Wong*[a,b]

[a] *Department of Chemistry, State University of New York at Stony Brook, New York 11794-3400, USA. E-mail: sswong@notes.cc.sunysb.edu; Tel: +1 631 632 1703*

[b] *Materials and Chemical Sciences Department, Brookhaven National Laboratory, Building 480, Upton, New York 11973, USA. E-mail: sswong@bnl.gov; Tel: +1 631 344 3178*

Received (in Cambridge, UK) 2nd July 2004, Accepted 7th September 2004
First published as an Advance Article on the web 13th October 2004

Multiferroic bismuth ferrite ($BiFeO_3$) nanotubes have been synthesized using a modified template methodology and characterized by a number of techniques, including XRD, SEM, TEM, HRTEM as well as EDX and SAED.

One-dimensional (1D) nanostructures, such as nanowires, nanorods, and nanotubes, have become the focus of studies because of their unique size-dependent properties and their relevant applications in mesoscopic physics and nanoscale device fabrication.[1–3] We have recently synthesized 1D structures of ternary transition metal oxide materials such as $BaTiO_3$ and $SrTiO_3$.[4,5] By analogy, the production of magnetic materials at the nanoscale promises to be significant for technologies involving data storage density, quantum computing, spintronics, and technologies involving memory and sensor development.[6–8] In this manuscript, we focus on the synthesis of 1D structures of magnetoelectric multiferroics.[9,10] These materials possess a spontaneous polarization, magnetization, and piezoelectricity that can be switched on by an applied electric field, magnetic field, and elastic force or stress, respectively.

In particular, $BiFeO_3$ shows ferroelectricity with a high Curie temperature (T_C) of ~1103 K, and antiferromagnetic properties below a Néel temperature (T_N) of 643 K.[7] Structural analysis of $BiFeO_3$ indicates that it possesses a rhombohedrally distorted perovskite structure with R_{3c} symmetry ($a = b = c = 5.63$ Å, $\alpha = \beta = \gamma = 59.4°$) at room temperature.[11] In its bulk form, measurement of ferroelectric and transport properties in bismuth ferrite have been limited by leakage problems, likely due to low resistivity, defects, and non-stoichiometry issues. To address this problem, recent approaches have focused on developing novel structures of $BiFeO_3$.[7,12] For instance, thin films of $BiFeO_3$ show physical properties such as spontaneous polarization, saturation magnetization, and a piezoelectric response, that are significantly enhanced relative to that of the bulk.[7] In addition, $BiFeO_3$ nanoparticles have been synthesized by a sol–gel process using organic precursors in the presence of dilute nitric acid solution. Preliminary magnetic property measurements of these nanoparticles were performed, showing enhanced properties corresponding to reduction of size.[12]

To our knowledge, there have not been any viable syntheses of 1D nanostructures of $BiFeO_3$ reported. The fabrication of 1D nanostructures of $BiFeO_3$ is of fundamental importance in investigating size correlation of the basic physical properties of these materials, with implications for their device applications. In the current work, for the synthesis of $BiFeO_3$ nanotubes (NTs), we have employed a template-based technique[13,14] because of its practicality in the sol–gel process, its relative simplicity, and its prior versatility in the preparation of high aspect ratio nanostructures of ternary metal oxides.[15,16] As-prepared $BiFeO_3$ 1D NTs were subsequently characterized by a number of techniques, including XRD, SEM, TEM, HRTEM as well as EDX and SAED.

In a typical synthesis, $Bi(NO_3)_3{\cdot}5H_2O$ and $Fe(NO_3)_3{\cdot}9H_2O$ with a molar ratio of 1 : 1 were added successively to ethylene glycol.[17,18] The resulting mixture was stirred at 80 °C for 1 h, after which a transparent sol was recovered upon evaporation of the excess ethylene glycol. Droplets of the sol were deposited using a syringe onto a porous anodic alumina (AAO) template (Whatman Anodisc®) surface with application of pressure.[19] AAO membranes with different pore sizes, such as 200 nm and 100 nm, have been used. The resultant samples, *i.e.* AAO templates containing the $BiFeO_3$ precursors, were subsequently oven-dried at 100 °C for an hour, and then preheated to 400 °C for three separate runs at a ramp-rate of 5 °C min^{-1} in order to get rid of excess hydrocarbons and NO_x impurities. The sample was further annealed at 600 °C for 30 min. $BiFeO_3$ NTs were isolated after the removal of the AAO template, following its immersion in 6 M NaOH solution at room temperature for 24 h. Thereafter, to retrieve reasonable quantities of nanotubes, the base solution was diluted in several steps with distilled water and lastly ethanol. Tubes were collected by centrifugation.

Fig. 1 shows scanning electron microscopy (SEM) images revealing the morphologies of $BiFeO_3$ NTs. Figs. 1A and 1B illustrate as-prepared $BiFeO_3$ NTs, grown in AAO membranes having 200 nm and 100 nm sized pores, respectively. The micrographs show dispersed individual $BiFeO_3$ NTs as well as some degree of NT bundling. It is evident that $BiFeO_3$ NTs generated from AAO membranes having pore sizes of 200 nm (Fig. 1A), mainly consist of straight and smooth structures with relatively few extraneous particulate debris. These tubes have outer diameters in the range of 240 to 300 nm, with lengths ranging from several microns to as much as 50 μm, corresponding to the entire length of the template membranes used. In the case of $BiFeO_3$ NTs generated from 100 nm diameter pores (Fig. 1B), the lengths of the NTs are not only understandably shorter but also more irregular and polydisperse. Their lengths attain several microns at best with diameters in the range of 140 to 180 nm. Tubular morphologies show a higher degree of roughness, as compared with those of $BiFeO_3$ NTs possessing larger diameters. The larger diameters of NTs can be presumably ascribed to larger internal diameters than surface ones of AAO membranes used.[19,20]

Figs. 2A and 2B illustrate transmission electron microscopy (TEM) images of an individual NT, generated from the alumina membrane with 100 nm and 200 nm diameter pores, respectively.

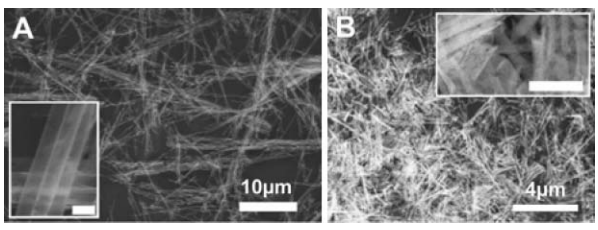

Fig. 1 SEM images of $BiFeO_3$ nanotubes (NTs) prepared in alumina membranes with 200 nm (A) and 100 nm (B) diameter pores, respectively. The insets of (A) and (B) show higher magnification images of as-prepared $BiFeO_3$ NTs, respectively. Scale bars in the insets of (A) and (B) indicate 500 nm.

† Electronic supplementary information (ESI) available: experimental details, powder X-ray diffraction (XRD) measurements, SEM data on bulk samples, and SQUID results. See http://www.rsc.org/suppdata/cc/b4/b409988e/

DOI: 10.1039/b409988e

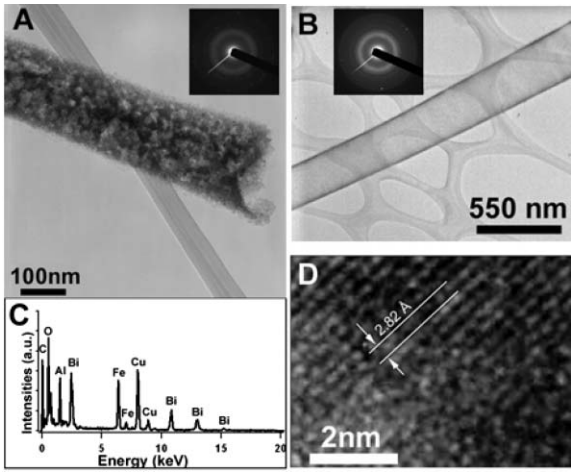

Fig. 2 TEM images of individual $BiFeO_3$ nanotubes (NTs) prepared in alumina membranes with 100 nm (A) and 200 nm (B) diameter pores, respectively. Insets of (A) and (B) are the corresponding SAED patterns of the individual NTs, respectively. (C) EDX data indicate that this individual NT is composed of Bi, Fe, and O and contains an Al impurity. The Cu and C peaks originate from the TEM grid. (D) HRTEM image of $BiFeO_3$ NTs generated from a template having 200 nm diameter pores.

The diameters are consistent with measurements from SEM data. EDX data (Fig. 2C) show the expected elemental signals of NTs arising from Bi, Fe, and O. We do observe varying intensities of Al peaks, ascribed to residue from the template. Even though both tubes have similar levels of Al layers on their surface, the discrepancies between the morphologies of each tube can be clearly seen. Fig. 2B shows straight and relatively smooth structures, while Fig. 2A indicates that straight but relatively rough and irregular structures are observed. The wall thickness for a $BiFeO_3$ NT obtained from the template with 200 nm diameter pores was $\sim$10 nm (Fig. 2B). Not surprisingly, analogous measurements for the $BiFeO_3$ NT generated from 100 nm diameter pores could not be properly obtained due to the roughness of the tube surface (Fig. 2A). Precedence for the observation of this type of morphology has been found with Co_3O_4 fibers synthesized using a sol–gel process.[21]

Selected area electron diffraction (SAED) data taken from each individual $BiFeO_3$ NT show identical ring patterns. The broad continuous ring patterns in the insets of Figs. 2A and 2B validate our view that the generated $BiFeO_3$ NTs consist of polycrystalline as well as amorphous states. HRTEM images further confirm the crystalline nature and composition of our as-prepared NTs. Fig. 2D shows a typical crystalline domain with an interplanar spacing of about 2.82 Å, which corresponds to the (110) ring in the SAED spectrum.

The purity and crystallinity of both the $BiFeO_3$ bulk and NT samples were examined using powder XRD (Fig. SI, part A; see ESI†). Very few if any impurity peaks were present in the bulk samples, prepared by an identical experimental protocol. Peaks can be indexed to the rhombohedral structure of $BiFeO_3$ which is in good agreement with literature results (*i.e.* JCPDS#20-0169). The XRD pattern of $BiFeO_3$ NTs is also shown for comparison and is in agreement with bulk and reference data. We note that since the template synthesis method produces relatively small amounts of confined nanostructures for XRD, data for the $BiFeO_3$ NTs were obtained indirectly (Fig. SI, part B; see ESI†) by subtracting the signal due to the alumina template from that of the template/$BiFeO_3$ sample itself.

In this work, to overcome the lack of wettability of the template by the sol, we employed a pressure-filter technique to force reagents into the pores.[19,20] Hence, the nature of the wetting of the precursor sol on the inner surface of the template membrane likely had a substantial effect on the morphology of the final products. For example, the duration of sol deposition as well as the viscosity of the sol itself are all important factors in considering interactions of sol constituents with the template membranes.[22] That is, the difference in morphology of the tubes synthesized in 100 *vs.* 200 nm pore-sized templates could have arisen not only from differential chemical interactions of the various sol constituents deposited with the pore walls themselves but also from contrasting geometric configurations of the sol constituent molecules within each individual template membrane, induced by spatial constraints. Moreover, as the nucleation of the $BiFeO_3$ particles likely starts from sites randomly located on the wall of the template, the net effect would be formation of polycrystalline $BiFeO_3$ NTs, consistent with the SAED and HRTEM results observed.

This current work demonstrates the first reported synthesis of 1D multiferroic $BiFeO_3$ nanotubes, using a pressure-filter variation of a template synthesis involving the sol–gel technique. The generation of $BiFeO_3$ nanotubes will be relevant for the design of future nanoscale building blocks for soft magnetic materials with applications in transformers and inductors. Future research will focus on property (such as ferroelectric, ferromagnetic, and ferroelastic) measurements of these $BiFeO_3$ NTs to determine the net effect of morphology.

We acknowledge support of this work through the US Department of Energy under contract number DE-AC02-98CH10886, the National Science Foundation (CAREER award DMR-0348239), and the donors of the ACS-PRF. SSW thanks 3M for a non-tenured faculty award. Dr James Quinn is acknowledged for his help with SEM and TEM results. We are grateful to Dr Arnold Moodenbaugh for preliminary SQUID data. We also thank Prof. Jianyu Huang for his assistance with HRTEM results. We acknowledge S. Banerjee and T. Hemraj-Benny for thoughtful comments.

Notes and references

1 Y. Xia, P. Yang, Y. Sun, Y. Wu, B. Mayers, B. Gates, Y. Yin, F. Kim and H. Yan, *Adv. Mater.*, 2003, **15**, 353.
2 G. R. Patzke, F. Krumeich and R. Nesper, *Angew. Chem., Int. Ed.*, 2002, **41**, 2446.
3 C. N. R. Rao and M. Nath, *Dalton Trans.*, 2003, 1.
4 Y. Mao, S. Banerjee and S. S. Wong, *Chem. Commun.*, 2003, 408.
5 Y. Mao, S. Banerjee and S. S. Wong, *J. Am. Chem. Soc.*, 2003, **125**, 15718.
6 H. Schmid, *Ferroelectrics*, 1999, **221**, 9.
7 J. Wang, J. B. Neaton, H. Zheng, V. Nagarajan, S. B. Ogale, B. Liu, D. Viehland, V. Vaithyanathan, D. G. Schlom, U. V. Waghmare, N. A. Spaldin, K. M. Rabe, M. Wuttig and R. Ramesh, *Science*, 2003, **299**, 1719.
8 M. Fiebig, T. Lottermoser, D. Fröhlich, A. V. Goltsev and R. V. Pisarev, *Nature*, 2002, **419**, 818.
9 H. Schmid, *Ferroelectrics*, 1994, **162**, 317.
10 N. A. Hill, *J. Phys. Chem. B*, 2000, **104**, 6694.
11 F. Kubel and H. Schmid, *Acta Crystallogr., Sect. B*, 1990, **46**, 698.
12 J. Li, H. He, F. Lü, Y. Duan and D. Song, *Mater. Res. Soc. Symp. Proc.*, 2002, **676**, Y7.7.1.
13 C. R. Martin, *Science*, 1994, **266**, 1961.
14 C. R. Martin, *Acc. Chem. Res.*, 1995, **28**, 61.
15 B. A. Hernandez, K.-S. Chang, E. R. Fisher and P. K. Dorhout, *Chem. Mater.*, 2002, **14**, 480.
16 S. J. Limmer, S. Seraji, M. J. Forbess, Y. Wu, T. P. Chou, C. Nguyen and G. Cao, *Adv. Mater.*, 2001, **13**, 1269.
17 T. Wada, A. Kajima, M. Inoue, T. Fujii and K. I. Arai, *Mater. Sci. Eng., A*, 1996, **217**(218), 414.
18 K. Toshimitsu, O. Shin-ichi and H. Dazuhito, *J. Phys. Chem. Solids*, 2003, **64**, 391.
19 M. Steinhart, J. H. Wendorff, A. Greiner, R. B. Wehrspohn, K. Nielsch, J. Schilling, J. Choi and U. Gösele, *Science*, 2002, **296**, 1997.
20 S. Ai, G. Lu, Q. He and J. Li, *J. Am. Chem. Soc.*, 2003, **125**, 11140.
21 B. B. Lakshmi, P. K. Dorhout and C. R. Martin, *Chem. Mater.*, 1997, **9**, 857.
22 M. Steinhart, R. B. Wehrspohn, U. Gösele and J. H. Wendorff, *Angew. Chem., Int. Ed.*, 2004, **43**, 1334.